

distributions of the two momentum states are not the same even though each momentum state contains the same total number of atoms (Fig. 2B). Consequently, when the two momentum states are combined with successive π and $\pi/2$ Bragg pulses, it is not possible to establish completely constructive or completely destructive interference. Three-dimensional numerical simulations that take into account the difference in the atomic density distributions (Fig. 2B) predict the maximum contrast to be 78%, which is in good agreement with our measured contrast of 71(6)%. This is to be compared to a Mach-Zehnder BEC interferometer (100% contrast) (7) that splits the condensate into two momentum states with identical density distributions, using a single $\pi/2$ Bragg pulse. The corrected maximum contrast of 78% implies that 83(14)% of the amplified wave is phase-coherent with the initial seed.

The phase-coherent matter-wave amplifier presented here is capable of amplifying a matter wave whose momentum p is in the range $0 < p < 2\hbar k$, provided the phase-matching condition is respected. If ϕ is the angle between the direction of propagation of the superradiance beam and that of the seed matter wave, the phase-matching condition becomes $p = 2\hbar k \cos\phi$. This condition is relaxed by the momentum spread of the source condensate, which, for a particular choice of ϕ , can be thought of as the matter-wave amplifier bandwidth.

In the present experiment, both the Bragg and the superradiance pulses were illuminated along the same direction. If we injected a small fraction of atoms along a different direction, we would be able to study mode competition in the matter-wave amplification process. One could use phase-coherent matter-wave amplification to enhance the number of atoms in atom lithography or holography (17) experiments in order to reduce signal accumulation time. Furthermore, it should be possible to make a ring cavity for matter waves using multiple Bragg diffractions as mirrors. By combining such a matter-wave cavity and the phase-coherent amplification mechanism demonstrated here, it should be possible to construct a new type of high-brightness atom laser.

References and Notes

- B. G. Huth, *Appl. Phys. Lett.* **16**, 185 (1970).
- M. H. Anderson et al., *Science* **269**, 198 (1995).
- K. B. Davis et al., *Phys. Rev. Lett.* **75**, 3969 (1995).
- P. J. Martin et al., *Phys. Rev. Lett.* **60**, 515 (1988).
- M. Kozuma et al., *Phys. Rev. Lett.* **82**, 871 (1999).
- D. M. Giltner, R. W. McGowan, S. A. Lee, *Phys. Rev. Lett.* **75**, 2638 (1995).
- Y. Torii et al., in preparation. Preprint available at <http://xxx.lanl.gov/abs/cond-mat/9908160> (1999).
- M.-O. Mewes et al., *Phys. Rev. Lett.* **78**, 582 (1997).
- B. P. Anderson and M. A. Kasevich, *Science* **282**, 1686 (1998). Unlike other atom lasers, in this work atoms in the same magnetic state tunnel out of a one-dimensional optical standing wave potential after the magnetic trap is switched off.
- I. Bloch, T. W. Hänsch, T. Esslinger, *Phys. Rev. Lett.* **82**, 3008 (1999).
- E. W. Hagley et al., *Science* **283**, 1706 (1999).
- S. Inouye et al., *Science* **285**, 571 (1999).
- C. K. Law and N. P. Bigelow, *Phys. Rev. A* **58**, 4791 (1998).
- M.-O. Mewes et al., *Phys. Rev. Lett.* **77**, 416 (1996).
- C. J. Myatt et al., *Opt. Lett.* **21**, 290 (1996).
- G. I. Peters and L. Allen, *J. Phys. A* **4**, 238 (1971).
- J. Fujita et al., *Nature* **380**, 691 (1996).
- Supported in part by a grant-in-aid from the Ministry of Education, Science, and Culture, and by Core Research for Evolutionary Science and Technology of the Japan Science and Technology Corporation. After submission of this manuscript, we learned that related work is being pursued at MIT.

28 September 1999; accepted 16 November 1999

Exciton Storage in Semiconductor Self-Assembled Quantum Dots

T. Lundstrom, W. Schoenfeld, H. Lee, P. M. Petroff*

Storage and retrieval of excitons were demonstrated with semiconductor self-assembled quantum dots (QDs). The optically generated excitons were dissociated and stored as separated electron-hole pairs in coupled QD pairs. A bias voltage restored the excitons, which recombined radiatively to provide a readout optical signal. The localization of the spatially separated electron-hole pair in QDs was responsible for the ultralong storage times, which were on the order of several seconds. The present limits of this optical storage medium are discussed.

Storing information in a cheap way will require ultrahigh packing densities as well as inexpensive self-assembling techniques and fast methods for writing and retrieving the information. Today, over 10 million atoms are required for storage of a single bit of information, but demands for faster addressing will require even smaller structures. Semiconductor QDs, which involve a few thousand atoms, may offer an attractive path toward achieving these goals. Charge storage devices based on the resistivity changes of a two-dimensional electron gas located near a layer of self-assembled QDs have been demonstrated at low temperature (1, 2). Quantum well (QW) devices designed for optical storage have been proposed and demonstrated (3, 4). Their storage characteristics are limited to short storage times (several hundred microseconds) at low temperature. Here, we present an approach for storing and retrieving information in QDs that uses an optical method and allows for exciton storage times of several seconds.

The QDs (5) are produced by molecular beam epitaxy (MBE). The size of the lens-shaped QDs (~30 to 40 nm in diameter and ~3 to 5 nm in height) is on the order of the electron wavelength, and the carrier energy levels are quantized. The sequential loading of electrons and holes and the three-dimensional confinement character of the carriers in the QDs have been demonstrated (6). The delta function density of states yields ultranarrow luminescence lines, and several studies have recently shown the importance and complexity of many body

effects in the relaxation processes involved in strongly excited QDs (7).

The device structure of QDs presented here is based on the splitting of an optically generated exciton into an electron-hole pair for the write cycle. The electron and hole are stored in closely spaced strain-coupled QD pairs. The effects of this strain coupling are to locally lower the band gap of the material and to localize the electron-hole pair (8). After the electron and hole are stored for a given time, an applied voltage bias can bring them together in the same QD, where they recombine radiatively for the readout cycle. We show exciton storage times at low temperature, which are more than a billion times longer than the exciton lifetime in normal QDs.

The central part of the device structure contains an InAs QD layer and a narrow GaAs QW that are separated by a thin AlAs layer. The 7% lattice mismatch between InAs and GaAs creates a strain field around the coherently strained InAs QDs. This strain field extends through the thin AlAs barrier into the narrow GaAs QW, where it creates a buried strain-induced QD (SIQD) (8). The cross-sectional micrograph from a transmission electron microscope (TEM) (Fig. 1) indicates that the strain field of the InAs QD extends to the GaAs QW, where it gives rise to a strain contrast. The QW thickness is chosen to ensure that its lowest electron energy level is above the X valley minimum in the AlAs barrier. This approach allows one to engineer the ladder of electronic levels shown in Fig. 2. The cascaded energy level structure ensures that the excitons created in the QW are efficiently separated into electron-hole pairs under the influence of an electric field. The relaxation of the electron from the SIQD to the X valley is a rapid process that occurs in a few

Materials Department, University of California, Santa Barbara, CA 93106, USA.

*To whom correspondence should be addressed. E-mail: petroff@engineering.ucsb.edu

REPORTS

picoseconds as was shown for QW structures (9). Further relaxation of the electron into the InAs QDs should also take place rapidly by tunneling or thermal excitation or both. In a QW structure, these relaxation processes have been shown to take place in 30 ps (9). This transfer process can be enhanced by inserting the structure into a metal/insulator/semiconductor device with an n^+ -doped GaAs layer serving as a back contact and a semitransparent Schottky top surface contact. An applied voltage bias will provide the exciton storage function to the device. The read process will be induced by a positive bias that will induce the hole tunneling from the SIQDs to the InAs QDs.

Several sample structures were grown by MBE on semi-insulating (001) GaAs substrates. After deposition of an AlAs/GaAs 40 (20 Å/20 Å) short-period superlattice for smoothing, a 1000 Å-thick n^+ GaAs (10^{18} cm^{-3}) back contact layer was grown, followed by an $\text{Al}_{0.5}\text{Ga}_{0.5}\text{As}$ (400 Å) barrier. Then the 68 Å-wide GaAs QW was deposited, and the InAs QDs layer was inserted in this QW. This was then followed by the deposition of a thin (60 or 100 Å) AlAs barrier, followed by a thin 25 Å GaAs QW, a 500 Å $\text{Al}_{0.5}\text{Ga}_{0.5}\text{As}$ barrier, a thin AlAs/GaAs 7 (20 Å/10 Å) short-period superlattice, and finally a 50 Å GaAs capping layer. A semitransparent Schottky contact was evaporated on the surface to provide the top gate.

The samples were mounted in a closed-cycle helium cryostat and cooled to a temperature below 5 K. An argon ion laser was used for excitation. The photoluminescence (PL) signal was collected through a 0.19-m single monochromator and detected by either a cooled photomultiplier tube or a liquid nitrogen-cooled silicon charge-coupled device camera. For the time-resolved PL experiments, an argon ion laser was modulated at 0.2 Hz with a pulse width of about 50 ms. For shorter time-resolved PL measurements, an acousto-optic modulator and a small aperture were used to create short ($<0.5 \mu\text{s}$) argon ion laser pulses. A multichannel scaler, whose smallest time bin width was 5 ns, was used to count and accumulate a time-dependent histogram of the single photons.

The photoluminescence of SIQDs for several optical pumping powers is labeled as B in Fig. 2. The luminescence lines shown on the PL spectra correspond to the transitions indicated on the band diagram schematic. The optically induced dipole created by the efficient separation of the electron and hole into adjacent QD-SIQD pairs induces a band bending that is responsible for the observed blue shift of the luminescence (Fig. 2) as the optical pumping power is increased (8). The

highest pumping power results in a saturation of the SIQD luminescence, and eventually the thin QW luminescence process dominates.

After the electron-hole pairs are loaded, they can be stored under various voltage bias conditions. For these experiments, we chose a 0-V bias, and the only built-in field is caused by the Fermi level alignment between the n^+ -doped back GaAs electrode and the semitransparent Schottky contact front electrode. A typical result of a time-resolved PL experiment is shown (Fig. 3) along with the corresponding schematic band diagrams of the device. The detection wave-

length was set to the peak of the QD luminescence (peak A at 1.25 eV in Fig. 2) and only a small number ($\sim 10\%$) of QDs contribute to the signal. During the laser pulse, we observed an intense emission from the QDs. Because a bias readout pulse of 0.5 V was applied 3 s after the write laser pulse, we observed luminescence from the QDs, indicating a successful readout of the stored charge. Without a laser excitation pulse, there was no detectable luminescence from the QDs (Fig. 3B). For this device structure, the optimal readout voltage bias pulse was found to be 0.5 V with a duration of 3 μs .

Fig. 1. (A) Schematic of the QD memory structure showing pairs of strain-coupled QDs and SIQDs. An electron-hole pair generated by optical pumping is shown. The electron is localized and stored in the InAs QD, and the hole is stored in the SIQD directly above the QD. (B) Cross-sectional TEM micrograph shows the strain contrast around the buried InAs QD and in the GaAs QW. g , Bragg reflection selected for this image.

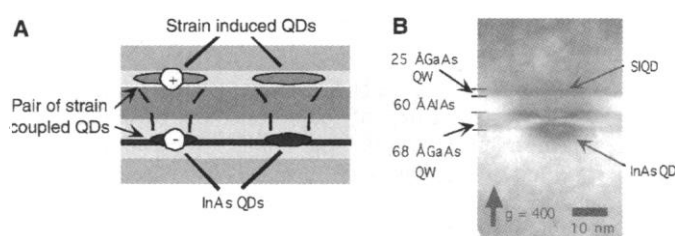


Fig. 2. (A) Low-temperature photoluminescence spectra of the QD memory sample for increasing pump powers (0.32, 1.3, 6.4, and 12 kW/cm^2). Dashed lines indicate the peak energy shifts; T , temperature; a.u., arbitrary unit. (B) Schematic band diagram showing the radiative transitions from the QDs (line A) and the spatially indirect recombination involving the SIQDs (line B).

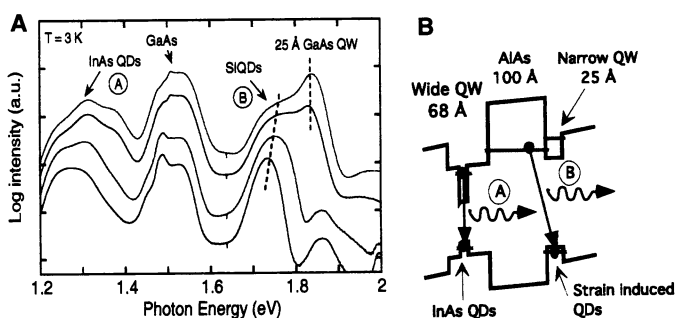
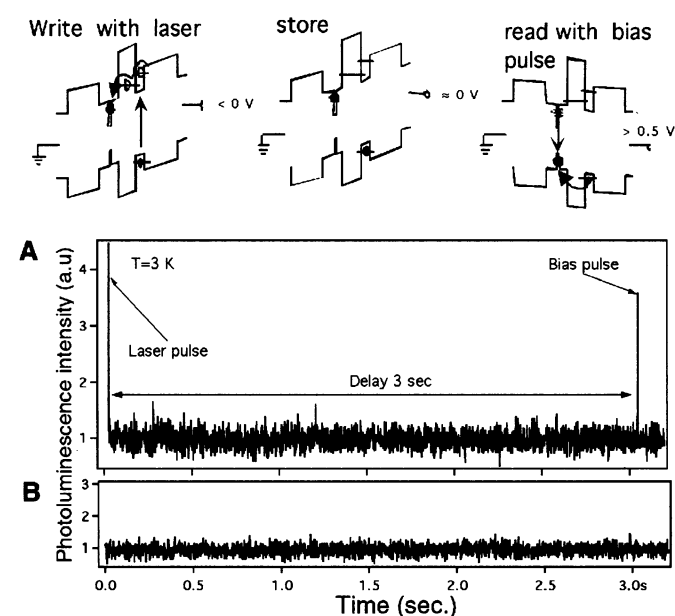


Fig. 3. Time-resolved luminescence from the QDs detected at 1.25 eV. (Top) The schematic band diagram of the device is shown for the write, store, and readout cycles of the device. (A) Writing the QD memory with a 2- μs laser pulse at 3 K and reading the memory with a short 0.5-V positive bias pulse. (B) No laser pulse but the same readout bias pulse is applied.



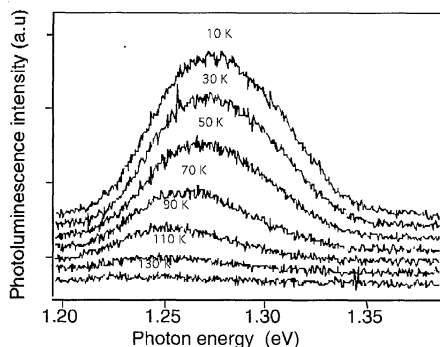


Fig. 4. Readout of the QD photoluminescence as a function of temperature for a forward bias of 0.5 V and a storage time of 100 ms.

The PL line shapes corresponding to the InAs QDs after a storage time of 100 ms for a range of temperatures between 3 and 130 K are shown (Fig. 4). The integrated PL signal in the temperature range from 10 to 130 K falls off with increasing temperature, and from this data, the measured activation energy for the exciton loss with temperature is ~ 20 meV. Analysis of the luminescence shift with increasing temperature suggests that the temperature dependence of the band gap, together with thermal evaporation of carriers out of the thinnest QDs in the structure, are responsible for the observed red shift. From the collected signal in Fig. 4, we obtained a rough estimate for the device efficiency of $\sim 10^{-9}$ at 10 K after storing the information for 100 ms. This number could be improved by loading the excitons while the device is under a negative bias of ~ -3 V. This will ensure a more efficient transfer of the electrons from the X level in the AlAs into the InAs QDs.

The time dependence of the stored luminescence at low temperature (Fig. 5) for a readout bias of 0.5 V shows a stored luminescence signal decay, I_s , which can be fitted to two

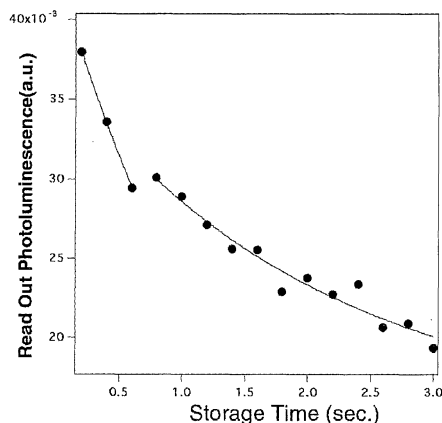


Fig. 5. Low-temperature (3 K) integrated intensity of the readout signal as function of time for a forward bias of 0.5 V. The lines are exponential fits to the data. The storage time extrapolated to the average noise level (on this scale, 6×10^{-3}) is ~ 10 s.

exponentials. For short storage times (5 μ s to 800 ms), $I_s \sim 4 \times 10^{-2}/e^{0.57t}$, but for long storage times (800 ms to 3 s), $I_s \sim 3 \times 10^{-2}/e^{0.18t}$, where t is the storage time in seconds. The stored signal decreases by $\sim 50\%$ in 3 s, and extrapolation to the noise level gives a storage time of nearly 10 s. The origin of these losses is still not clear, but several effects could be responsible for the decreasing readout signal. First, the overlap of the wave functions of electrons and holes could be important, and some of the stored spatially indirect excitons could be lost during the storage time. Second, carrier (hole) losses could occur by capture at deep levels in the AlAs barrier by tunneling during the storage cycle. Third, it is possible that some of the electrons stored in the InAs QDs could be recombining with the residual holes, because the MBE material has a carbon acceptor background concentration of $\sim 5 \times 10^{15}$ cm $^{-3}$.

The exciton storage times are remarkably long, $\sim 10^9$ times those of the exciton lifetimes in QDs ($1 - 5 \times 10^{-9}$ s). These long exciton storage times should also be compared to exciton lifetimes in n-doped/insulator/p-doped/insulator QW structures. Typical values of ~ 1 ms at 4 K have been reported (10), and in this case the structure does not exhibit a memory function. In type I-type II-coupled QW structures that do not contain QDs, exciton lifetimes of a few microseconds have been reported (9). The long storage times in the present QD structures are consistent with electron-hole pair localization in

the QD pairs and a low concentration of recombination centers in the QDs.

Much remains to be done to fully understand these long exciton lifetimes and to make use of the high density of QDs as an inexpensive storage medium. Nevertheless, writing and retrieving information using light and self-assembled QDs may offer substantial speed and power advantages for the next generation of devices.

References and Notes

1. J. J. Finley *et al.*, *Appl. Phys. Lett.* **73**, 2618 (1998).
2. G. Yusa and H. Sakaki, *Appl. Phys. Lett.* **70**, 345 (1997).
3. C. Roche *et al.*, *Phys. Rev. Lett.* **78**, 4099 (1997).
4. A. Wixforth, J. P. Kotthaus, W. Wegscheider, M. Bichler, *Science* **283**, 1292 (1999).
5. D. Leonard, M. Krishnamurthy, C. M. Reaves, S. P. DenBaars, P. M. Petroff, *Appl. Phys. Lett.* **63**, 3203 (1993).
6. M. Fricke, A. Lorke, J. P. Kotthaus, G. Medeiros-Ribeiro, P. M. Petroff, *Eur. Phys. Lett.* **36**, 197 (1996).
7. E. Dekel *et al.*, *Phys. Rev. Lett.* **80**, 4991 (1998); G. Abstreiter *et al.*, *Jpn. J. Appl. Phys.* **38**, 449 (1999).
8. W. Schoenfeld, T. Lundstrom, P. M. Petroff, *Appl. Phys. Lett.* **74**, 2194 (1999).
9. J. Feldmann *et al.*, *Solid State Commun.* **83**, 245 (1992).
10. W. Rehm, P. Ruden, G. H. Döhler, K. Ploog, *Phys. Rev. B* **28**, 5937 (1983); G. H. Döhler, in *Properties of III-V Superlattices and Quantum Wells*, P. Bhattacharya, Ed. (Electronic Materials Information Service, Stevenage, UK, 1996), vol. 15, p. 11.
11. Supported by the U.S. Army Research Office (contract number DAA G56-97-1-1301) and by QUEST, an NSF Science and Technology Center (DMR no. 91-20007).

24 August 1999; accepted 27 October 1999

Experimental Tunneling Ratchets

H. Linke,^{1*} T. E. Humphrey,¹ A. Löfgren,² A. O. Sushkov,¹
R. Newbury,¹ R. P. Taylor,¹ P. Omling²

Adiabatically rocked electron ratchets, defined by quantum confinement in semiconductor heterostructures, were experimentally studied in a regime where tunneling contributed to the particle flow. The rocking-induced electron flow reverses direction as a function of temperature. This result confirms a recent prediction of fundamentally different behavior of classical versus quantum ratchets. A wave-mechanical model reproduced the temperature-induced current reversal and provides an intuitive explanation.

In the absence of any net macroscopic forces, asymmetric potentials can be used to induce a particle flow when subjected to external fluctuations (1–5). Referred to as ratchets, their operation has been proposed as the underlying physical principle of molecular motors in biological systems (1, 2, 5–7), such as the

myosin-actin system that affects muscle contraction (8, 9). Fluctuation-induced particle current has also been observed in artificial ratchets (10–16). When tunneling contributes to the particle flow in an adiabatically rocked ratchet, it has been predicted that the current direction will depend on temperature (17). Here we use quantum confinement to define an electron ratchet in a semiconductor nanostructure. We find that the two contributions to the rocking-induced current (tunneling through and excitation over the ratchet's energy barrier) flow in opposite directions.

¹School of Physics, University of New South Wales, Sydney 2052, Australia. ²Division of Solid State Physics, Lund University, Box 118, 221 00 Lund, Sweden.

*To whom correspondence should be addressed. E-mail: hl@phys.unsw.edu.au